

Anticyclonic Eddies in the Alaskan Stream

HIROMICHI UENO,* HOWARD J. FREELAND,⁺ WILLIAM R. CRAWFORD,⁺ HIROJI ONISHI,[#]
EITAROU OKA,^{*,@} KANAKO SATO,^{*} AND TOSHIO SUGA^{*,&}

**Institute of Observational Research for Global Change, Japan Agency for Marine-Earth Science and Technology,
Yokosuka, Kanagawa, Japan*

+ Institute of Ocean Sciences, Fisheries and Oceans Canada, Sidney, British Columbia, Canada

*#Division of Marine Bioresource and Environmental Science, Graduate School of Fisheries Science,
Hokkaido University, Hakodate, Japan*

@ Ocean Research Institute, University of Tokyo, Tokyo, Japan

& Department of Geophysics, Graduate School of Science, Tohoku University, Sendai, Japan

(Manuscript received 7 November 2007, in final form 21 October 2008)

ABSTRACT

Anticyclonic eddies propagating southwestward in the Alaskan Stream (AS) were investigated through analysis of altimetry data from satellite observations during 1992–2006 and hydrographic data from profiling float observations during 2001–06. Fifteen long-lived eddies were identified and categorized based on their area of first appearance. Three eddies were present at the beginning of the satellite observations; another three formed in the eastern Gulf of Alaska off Sitka, Alaska; and four were first detected at the head of the Gulf of Alaska near Yakutat, Alaska. The other five eddies formed along the AS between 157° and 169°W, and were named AS eddies. While the eddies that formed in the Gulf of Alaska mainly decayed before exiting the Gulf of Alaska, the AS eddies mostly crossed the 180° meridian and reached the western subarctic gyre. Four of five AS eddies formed under negative or weakly positive wind stress curls, which possibly caused AS separation from the coast. Comparison of eddy propagation speeds in the AS with the bottom slope showed that eddies propagated faster over steeper slopes, although eddy speeds were slower than those predicted by the topographic planetary wave dispersion relation. An AS eddy was observed by profiling floats in the western subarctic gyre after it detached from the AS. Intermediate-layer water near the eddy center had low potential vorticity compared with the surrounding water, suggesting that AS eddies provided the western subarctic gyre with water just south of the Aleutian Islands.

1. Introduction

The Alaskan Stream (AS; Fig. 1) is a subarctic western boundary current in the North Pacific Ocean, flowing southwestward from the head of the Gulf of Alaska (~145°W) along the Alaskan Peninsula and the Aleutian Islands (Reed and Schumacher 1986). The AS serves as a connection between the Alaskan gyre, the western subarctic gyre, and the Bering Sea gyre, playing an important role in the volume, heat, and freshwater transports in the subarctic North Pacific (Onishi and Ohtani 1999).

The AS and the Alaska Current, a broad northward current flowing in the eastern Gulf of Alaska, are known

to involve offshore meanders and anticyclonic eddies (both are referred to as eddies in this paper). In the Gulf of Alaska, three types of eddies have been identified based on their formation region. Haida eddies form in winter off the west coast of the Queen Charlotte Islands (~53°N) and move mostly westward to the central Gulf of Alaska (Crawford and Whitney 1999; Crawford 2002). Sitka eddies appear off Sitka, Alaska (~57°N) (Tabata 1982). They move mostly westward (Gower 1989; Crawford 2002), while some of them move northwestward and become embedded in the AS (Crawford et al. 2000; identified as CCF2000 in Table 1). Yakutat eddies form at the head of the Gulf of Alaska (141°–144°W) near Yakutat, Alaska, and propagate southwestward in the AS along the northwestern continental margin of the Gulf of Alaska (Ladd et al. 2005b, 2007).

Previous studies reported that eddies in the Gulf of Alaska had a significant impact on the heat, freshwater,

Corresponding author address: Hiromichi Ueno, Institute of Observational Research for Global Change, Japan Agency for Marine-Earth Science and Technology, 2-15 Natsushima-cho, Yokosuka, Kanagawa 237-0061, Japan.
E-mail: uenohiro@jamstec.go.jp

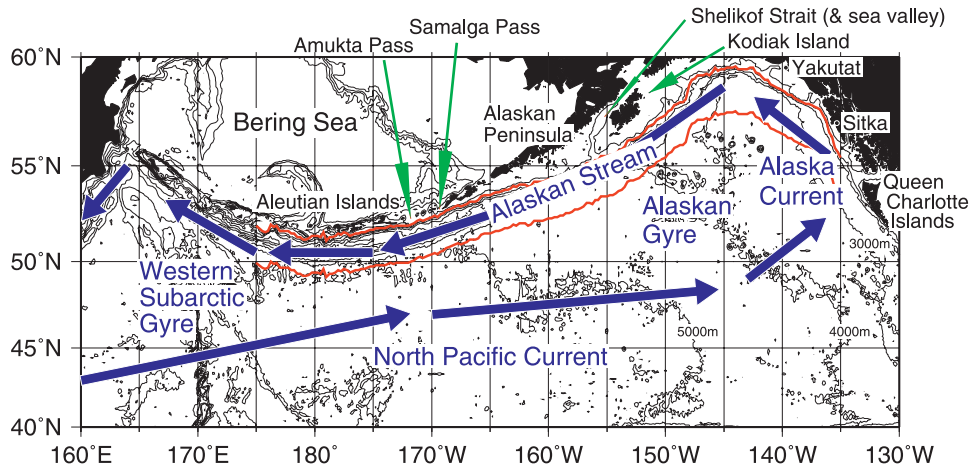


FIG. 1. Schematic representation for the currents of the subarctic North Pacific. Bathymetric contours are 200 m and every 1000 m, starting from 1000 m. Thick red lines are the 1000-m depth contours between 175°E and 135°W, and the line 2° south of it. The area between the two lines corresponds to the area where the SLA was averaged in Fig. 3.

nutrient, and biota exchange between the shelf region and the offshore region. Haida eddies and some Sitka eddies, which propagate westward to the central Gulf of Alaska, carry warm, fresh, and nutrient-rich coastal water containing biota in the shelf region to the central Gulf of Alaska by trapping shelf water at the eddy center and by advection in the outer ring of the eddy (Crawford 2002; Mackas and Galbraith 2002; Whitney and Robert 2002; Crawford et al. 2005). The deep-sea region of the eastern subarctic North Pacific is a high-nutrient, low-chlorophyll (HNLC) environment (Martin et al. 1989; Boyd et al. 1998; Harrison et al. 1999; Wong et al. 2002), and the primary production is limited by iron (Boyd et al. 2004). Haida eddies supply the Alaskan gyre with iron-rich coastal waters (Johnson et al. 2005), and so they may play a crucial role in the productivity of the Alaskan gyre.

Yakutat eddies and some Sitka eddies propagating southwestward in the AS in the northwestern Gulf of Alaska also affect the water exchange between the shelf and offshore regions. Okkonen et al. (2003) indicated that these eddies altered the structure of the shelf break front, and in so doing, influenced the shelf-slope exchange of biota and water mass properties. Ladd et al. (2005c) and Crawford et al. (2007) showed that Sitka and Yakutat eddies influenced cross-shelf exchange by trapping coastal water in their interiors and propagating offshore, and also by interfering with the slope circulation and resulting in cross-shelf flow.

Some of the eddies in the Gulf of Alaska were reported to go out of the Gulf of Alaska and propagate downstream in the AS along the Aleutian Islands. Crawford et al. (2000) analyzed Ocean Topography Experiment (TOPEX)/Poseidon altimeter data from 1992

to 1998 and detected six long-lived eddies in the AS. One of these eddies propagated from the Gulf of Alaska to 180°, although its formation was not observed due to data limitations. Ladd et al. (2005b, 2007) demonstrated using altimetry data during 2001–06 that a Sitka eddy propagated along the AS and reached just east of 180°, with a lifetime exceeding 5 yr. Okkonen (1992) used *Geosat* altimeter data in 1987 and 1988 to describe an eddy in the AS that crossed the 180° meridian and entered the western subarctic gyre, although the eddy was traced only between 175°W and 174°E and its formation and decay were unclear because of data limitations. Eddies in the AS were also seen in a worldwide map of eddy trajectories from TOPEX/Poseidon and *European Remote Sensing Satellites-1* and *-2 (ERS-1/2)* altimeter datasets in Chelton et al. (2007), but individual trajectories were not demonstrated in their analysis. Rogachev et al. (2007) investigated eddies in the western subarctic gyre, which were mainly formed at 170°–175°E along the Aleutian Islands, and indicated that they supplied the East Kamchatka Current with heat.

Eddies in the AS along the Aleutian Islands could have a significant impact on the heat, freshwater, nutrient, and biota exchange between the coastal area south of the Aleutian Islands and the offshore region in the western and central subarctic North Pacific, in a similar manner to the eddies in the Gulf of Alaska. In addition, eddies south of the Aleutian Islands were suggested to drive the flow between the North Pacific and the Bering Sea (Okkonen 1996). However, comprehensive study of eddies in the AS along the Aleutian Islands from their formation to decay has not been performed using long-term data.

In this study we use satellite altimeter data from October 1992 to December 2006 to examine the formation, evolution, and termination of eddies in the AS and those detached from the AS. We also use hydrographic data from Argo profiling floats to study the structure of eddies in the AS. Our analysis of eddies, based on 14 yr of altimetry observations as well as float observations, would improve our understanding of the influence of eddies in the AS on the physical and biogeochemical fields in the western and central subarctic North Pacific as well as in the Bering Sea.

2. Data and methods

We used delayed-time data of sea level anomaly (SLA) and absolute dynamic topography (ADT) produced by the Segment Sol Multimissions d'Altimétrie, d'Orbitographie et de Localisation Précise/Multimission Altimeter Data Processing System (SSALTO/DUACS) from TOPEX/Poseidon, the *Geosat Follow-On (GFO)*, *Jason-1*, *ERS-1/2*, and *Environmental Satellite (Envisat)* observations, distributed by the Archiving, Validation and Interpretation of Satellite Oceanographic (AVISO) data center of Collecte Localisation Satellites (CLS) (Le Traon et al. 2003; Pascual et al. 2006; AVISO 2007). The temporal and spatial resolutions are 7 days and $0.25^\circ \times 0.25^\circ$, respectively, and we analyzed the data from 14 October 1992 to 27 December 2006. The spatial mean state of the subarctic North Pacific north of 45°N , except for the marginal seas, was removed from each weekly map of the SLA to compensate for seasonal steric effects. The effective temporal resolution is determined by the repeat times of satellites. The ERS and *Envisat* tracks repeat every 35 days, the longest interval of all altimeter satellites. These satellites provide the best spatial resolution.

We also used temperature and salinity profiles recorded by Argo floats (Argo Science Team 2001) in the North Pacific north of 40°N during 2001–06 to study the hydrographic structure of eddies in the AS. The real-time quality-controlled float data were downloaded from the ftp site of Argo Global Data Assembly Center (information online at <ftp://usgodae1.fnmoc.navy.mil/pub/outgoing/argo> and <ftp://ftp.ifremer.fr/ifremer/argo>). From these data, defective temperature and salinity profiles, such as those with measurements flagged as bad and those lacking intermediate layers for certain depths, were eliminated, following the procedures of Oka et al. (2007).

Daily wind stress data and monthly evaporation and precipitation (from the latent heat flux) data from the National Centers for Environmental Prediction–National Center for Atmospheric Research (NCEP–NCAR) re-

analysis (Kalnay et al. 1996) were also used. Wind stress data were analyzed after applying a 30-day running mean at each grid point. We also used bottom topography data of $2'$ gridded elevations/bathymetry for the world (ETOPO2v2; National Geophysical Data Center 2006).

Anticyclonic eddies in the AS were detected as SLA maxima, neglecting eddies whose maximum SLAs were less than 5 cm. In this study, we concentrated on the eddies that first appeared east of 180° , persisted for at least 6 months, and propagated southwestward to the west of 155°W along the AS. The eddies are identified based on the year of the first appearance (e.g., eddy 96a). When the main part of the eddy detaches from the AS, the detached eddy is called, for example, eddy 96a0 and the portion remaining in the AS is called, for example, eddy 96a1. The added number increases every time a detachment occurs.

The weekly propagation speed along the 1000-m depth contour for each eddy was evaluated from the eddy locations 4 weeks before and after, so that the typical eddy propagation distance during each 8-week period was long enough compared with the spatial resolution of SLA ($0.25^\circ \times 0.25^\circ$). The propagation speed was evaluated only for eddies that were located within 2° south of the 1000-m depth contour (Fig. 1) between 180° and 145°W , and not for those detached from the AS. As the result, 1084 eddy propagation speed data points were obtained.

The sea bottom slope and surface AS velocity at each weekly eddy location were evaluated as follows. We averaged the original bottom topography data with a resolution of $2' \times 2'$ in $0.1^\circ \times 0.1^\circ$ grid boxes, and calculated the bottom slope (gradient) normal to 1000-m depth contour for each grid with a horizontal scale of 50 km, neglecting bottom topography deeper than 5000 m. The bottom slope for each weekly eddy location was then calculated as a 8-week average of bottom slope along the eddy trajectory. The alongshore surface AS velocity for each weekly eddy location was evaluated as an average of the surface AS velocities at the longitudes of 2.5° west and 2.5° east of the eddy location to avoid the influence of the eddy on the AS velocity. Surface AS velocity at each longitude was evaluated as the highest alongshore surface velocity within 2° south of the 1000-m depth contour (Fig. 1), using ADT data and assuming geostrophy.

We evaluated potential vorticity (PV) as $\rho^{-1}f\Delta\sigma_\theta/\Delta z$, where f is the Coriolis parameter, ρ is density, and $\Delta\sigma_\theta/\Delta z$ is vertical gradient of potential density. The Δz was set to be 50 m. For the eddies whose PVs were evaluated, the magnitude of the relative vorticity was $O(10^{-5} \text{ s}^{-1})$ at the surface, which was one order smaller than f . Therefore, we neglected relative vorticity in this study.

3. Results

a. Formation, propagation, and termination of eddies in the Alaskan Stream

During the analysis period, 15 long-lived eddies were observed in the Alaska Current and the AS (Fig. 2, Table 1). These eddies formed along the AS south of the Alaskan Peninsula and the Aleutian Islands as well as along the Alaska Current in the northeastern Gulf of Alaska, and propagated downstream along the AS. During the propagation, some eddies left the AS, and some separated into two or three eddies.

Eddies 92a, 92b, and 92c already existed on 14 October 1992, the beginning of the altimetry data, so their formation regions could not be identified. They propagated downstream in the AS to $\sim 180^\circ$ (eddies 92a and 92c) and to $\sim 170^\circ\text{W}$ (eddy 92b).

Eddies 96d, 00a, and 04a were first observed in the northeastern Gulf of Alaska off Sitka, and were considered to be Sitka eddies. They propagated northward after their formation, became embedded in the AS, and propagated southwestward along the AS. Eddy 96d detached from the AS around 152°W and moved southwestward while decaying. After the detachment, a small eddy was left in the AS, but it soon vanished. Eddy 00a propagated to $\sim 180^\circ$ along the AS, while detaching an isolated eddy around 171°W . The detached eddy moved southwestward and decayed at 175°W . Eddy 04a propagated to $\sim 157^\circ\text{W}$, still existing at the end of our analysis period.

Eddies 95a, 96c, 99c, and 03a were first detected at the head of the Gulf of Alaska near Yakutat (Yakutat eddies), and propagated southwestward along the AS. Eddy 95a detached a small isolated eddy near 156°W ; both the detached and remaining eddies decayed rapidly. Eddy 96c stopped propagating and weakened near 157°W . It then propagated eastward to 155°W , was absorbed by the AS, and vanished. Eddy 99c decayed near 160°W . Eddy 03a detached an isolated eddy close to 155°W ; the eddy left in the AS still existed with an SLA higher than 40 cm at the end of the analysis period, while the detached eddy stayed near 155°W and decayed there. All isolated eddies detached from Sitka and Yakutat eddies in the AS moved less than 5° in longitude after their detachment, persisting for 1–16 months.

Eddies 96a, 96b, 99a, 99b, and 02a appeared along the AS between 157° and 169°W . The formation region of these eddies lies to the west of regions where Haida, Sitka, and Yakutat eddies form. We call these eddies Alaskan Stream (AS) eddies, following Okkonen et al. (2001) who detected eddy formation near 160°W in a numerical model. Crawford et al. (2000) first detected an AS eddy, eddy 96b (eddy 5 in their paper), in the

altimetry data, but did not discuss its lifetime behavior due to data limitations. In this study we detected five AS eddies and examined them from their formation to decay, revealing their behavior over their full lifetimes.

Eddy 96b first appeared at 158°W south of the Alaskan Peninsula and moved southwestward along the AS while increasing its maximum SLA up to 67 cm. It detached from the AS near 170°W and moved southwestward to 46°N , 179°E , a little beyond the 180° meridian. Eddy 99b also formed south of Alaskan Peninsula but decayed in ~ 10 months at 169°W . Eddy 96a formed at 163°W , the eastern edge of the Aleutian Islands, propagated westward to 175°E , and detached an isolated eddy at $\sim 170^\circ\text{W}$. Eddy 99a was first detected at 165°W south of Unimak Pass and moved westward while detaching two isolated eddies at $\sim 170^\circ\text{W}$ and $\sim 180^\circ$. The eddy left in the AS separated from the AS around 175°E . All three eddies born from eddy 99a (99a0, eastern; 99a1, middle; 99a2, western) moved southwestward away from the AS. Eddies 99a1 and 99a2 propagated deeply into the western subarctic gyre west of 180° . Eddy 02a first appeared at 169°W , moved westward along the AS, left the AS at $\sim 178^\circ\text{W}$, and propagated southwestward to 48°N , 175°E in the western subarctic gyre.

b. Behavioral aspects of eddies in the Alaskan Stream

Five of 15 long-lived eddies in the AS moved westward beyond 180° . One of these eddies (eddy 92c), which was present in the beginning of satellite altimetry observation, passed the 180° meridian by just 1° along the AS. The remaining four eddies (eddies 96a, 96b, 99a, and 02a) that crossed 180° and reached the western subarctic gyre were all AS eddies. This might be related to the formation region of AS eddies (157° – 169°W). East of the region, eddies in the AS (Sitka and Yakutat eddies) likely decayed (Fig. 2, Table 1).

All 15 long-lived eddies in the AS are seen in Fig. 3, the longitude–time diagram of the SLA along the Alaska Current and the AS. In addition to eddies shown in Fig. 2 (white dots), westward-propagating SLA maxima with a lifetime shorter than ~ 1 yr were frequently observed, particularly between 140° and 150°W , once to several times every year. Many of them disappeared in the Gulf of Alaska before reaching 155°W .

SLAs along the Alaska Current and the AS were lower during 1999–2004 than 1992–98 and 2005–06 (Fig. 3). During 1999–2003, fewer eddies were observed in the AS, although strong eddylike features were seen in the Gulf of Alaska near 145°W (Fig. 3), as indicated by Ladd (2007). Therefore, the fewer eddies in the AS might be due to relatively strong eddy decay (or weak eddy enhancement) in the western Gulf of Alaska during the period. Henson and Thomas (2008) indicated that

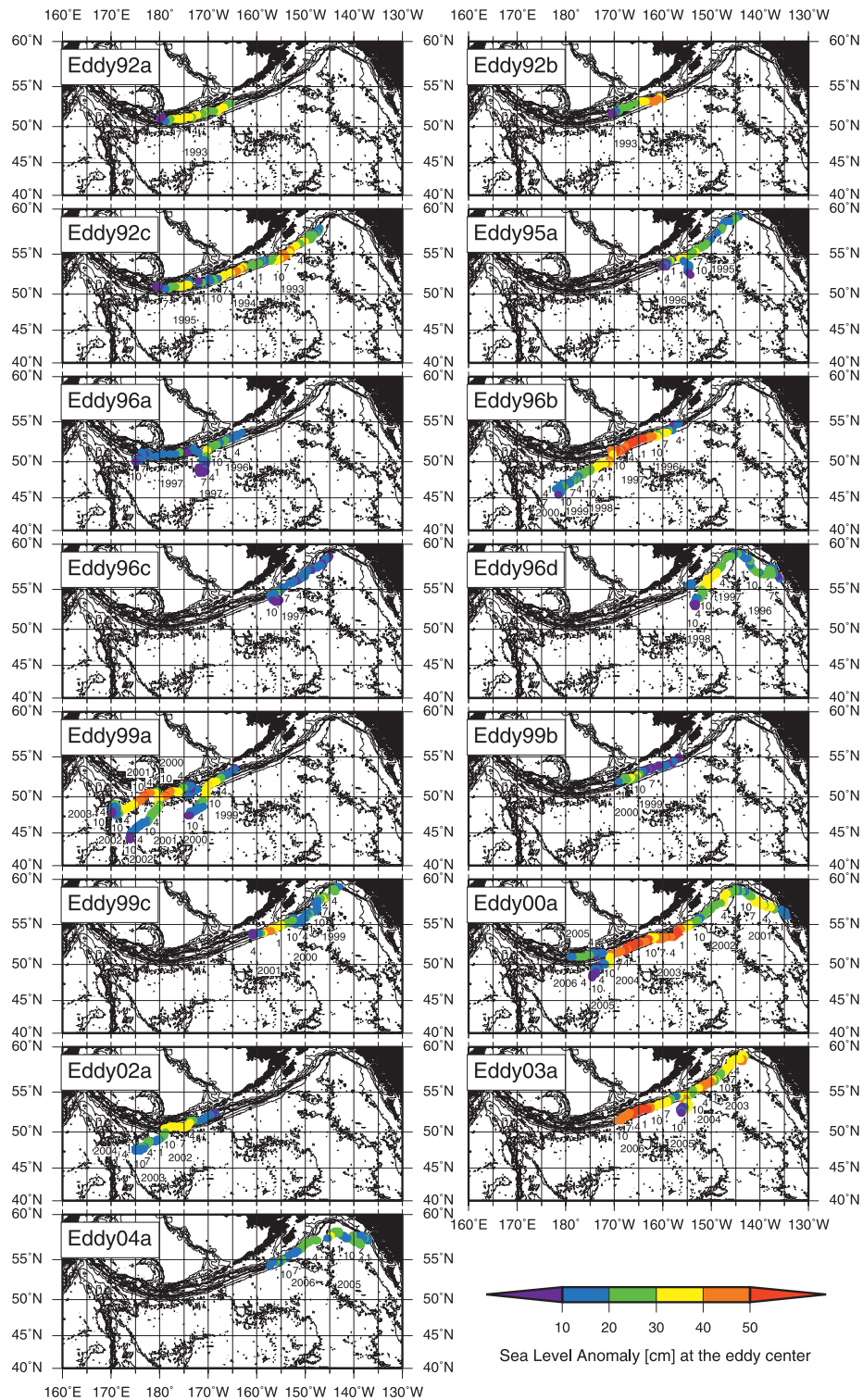


FIG. 2. Trajectories of long-lived eddies in the AS. Colors represent the SLA (cm) at the eddy center. Bathymetric contours are the same as in Fig. 1. The figures located just below or above the eddy trajectory indicate the month and year when the eddy was observed.

TABLE 1. Features of 15 long-lived eddies in the AS.

Eddy name	Day and location of first appearance	Last day and location of observation	Formation area	Previous studies
92a	Not identified	15 Sep 1993(51.00°N, 180.00°E)	N/A	Eddy 1 in CCF2000
92b	Not identified	21 Jul 1993(51.75°N, 170.50°W)	N/A	Eddy 2 in CCF2000
92c	Not identified	30 Aug 1995(51.00°N, 179.25°E)	N/A	Eddy 3 in CCF2000
95a	18 Jan 1995 (59.25°N, 144.25°W)	[0] 3 Apr 1996(52.50°N, 154.25°W) [1] 20 Mar 1996(53.50°N, 160.00°W)	Yakutat	Eddy 4 in CCF2000
96a	13 Mar 1996 (53.75°N, 163.00°W)	[0] 6 Aug 1997(48.50°N, 171.75°W); [1] 22 Oct 1997(50.00°N, 175.00°E)	AS	N/A
96b	13 Mar 1996 (54.75°N, 157.75°W)	5 Jul 2000(45.50°N, 178.50°E)	AS	Eddy 5 in CCF2000
96c	23 Oct 1996 (58.75°N, 145.00°W)	10 Dec 1997(53.75°N, 155.25°W)	Yakutat	N/A
96d	24 Jan 1996 (56.25°N, 136.00°W)	[0] 25 Nov 1998(53.00°N, 153.50°W) [1] 7 Jan 1998(55.50°N, 154.75°W)	Sitka	Eddy 6 in CCF2000
99a	3 Mar 1999 (53.75°N, 164.50°W)	[0] 13 Dec 2000(47.50°N, 174.25°W); [1] 20 Nov 2002(44.00°N, 174.00°E); [2] 25 Feb 2004(47.75°N, 170.25°E)	AS	N/A
99b	21 Apr 1999 (55.00°N, 156.75°W)	9 Feb 2000(52.00°N, 169.00°W)	AS	N/A
99c	10 Mar 1999 (59.25°N, 143.00°W)	2 May 2001(54.00°N, 161.00°W)	Yakutat	Eddy A in Okkonen et al. (2003)
00a	29 Nov 2000 (56.00°N, 134.50°W)	[0] 5 Jul 2006(48.25°N, 174.50°W); [1] 8 Jun 2005(51.00°N, 179.00°W)	Sitka	2001 eddy in Ladd et al. (2007)
02a	16 Jan 2002 (52.50°N, 168.50°W)	9 Jun 2004(47.50°N, 175.00°E)	AS	N/A
03a	8 Jan 2003 (59.00°N, 143.00°W)	[0] 22 Feb 2006(52.50°N, 156.25°W); [1] 27 Dec 2006(51.50°N, 169.50°W)	Yakutat	Yakutat eddy (Ladd et al. 2005b), 2003 eddy (Ladd et al. 2007)
04a	22 Dec 2004 (57.25°N, 137.00°W)	27 Dec 2006(54.25°N, 157.25°W)	Sitka	N/A

the area occupied by eddies was small during 1999–2002 in the AS between 142.5° and 160°W because the along-coast wind component was weak and thus unfavorable for downwelling along the eastern and northern coasts of the Gulf of Alaska during this period.

Occasionally, eddies appear to stop propagating for a while and amplify. Eddies 92c, 95a, 96c, 99c, 00a, and 03a stayed around 155°W for several months and amplified; three of them (eddies 95a, 96c, and 03a) detached from the AS (Figs. 2 and 3). Eddies 92c, 96a, 96b, 99a, and 00a stayed near 170°W for several months, intensified, and finally detached from the AS (except for eddy 92c). These behaviors might be related to the water exchange between the AS and the shelf/strait regions. This topic will be discussed in section 4b.

c. The structure of eddies in the Alaskan Stream

We further investigate the hydrographic structure of eddies in the AS using Argo profiling float data. In the Gulf of Alaska, hydrographic surveys across eddies in the AS have been conducted (Okkonen et al. 2003; Ladd et al. 2005b, 2007). Therefore, we restrict our analysis to the area west of ~160°W, where few ship-based studies

have sampled. In this longitude range, three eddies (00a, 02a, and 03a) were sampled by Argo floats. For each eddy, we composited all Argo float data observed near the eddy in time (< 3 days) and in space (< 220 km) (Figs. 4–6). Since seasonal variation is large near the sea surface, we here discuss the subsurface layer below 100-m depth.

Eddy 00a (Sitka eddy) was observed between 159° and 164°W from May to December 2003 by an Argo float while it was propagating westward in the AS (Fig. 4). At depths greater than 250 m, isopycnals, isotherms, and isohalines lowered toward the center of the eddy, similarly to Sitka eddies previously observed in the eastern Gulf of Alaska (e.g., Tabata 1982). The layer lowering was significant within ~70 km from the center, suggesting that this eddy had a diameter of ~140 km. The temperature–salinity (T–S) diagram shows two types of subsurface water with temperatures of 4°–5°C and 5°–6°C at 26.0–26.8 σ_θ (Fig. 4d). The former colder water, observed more than 80 km away from the eddy center, is considered to be the Ridge Domain Water in the Alaskan gyre (Musgrave et al. 1992) located outside of the eddy. Meanwhile, the

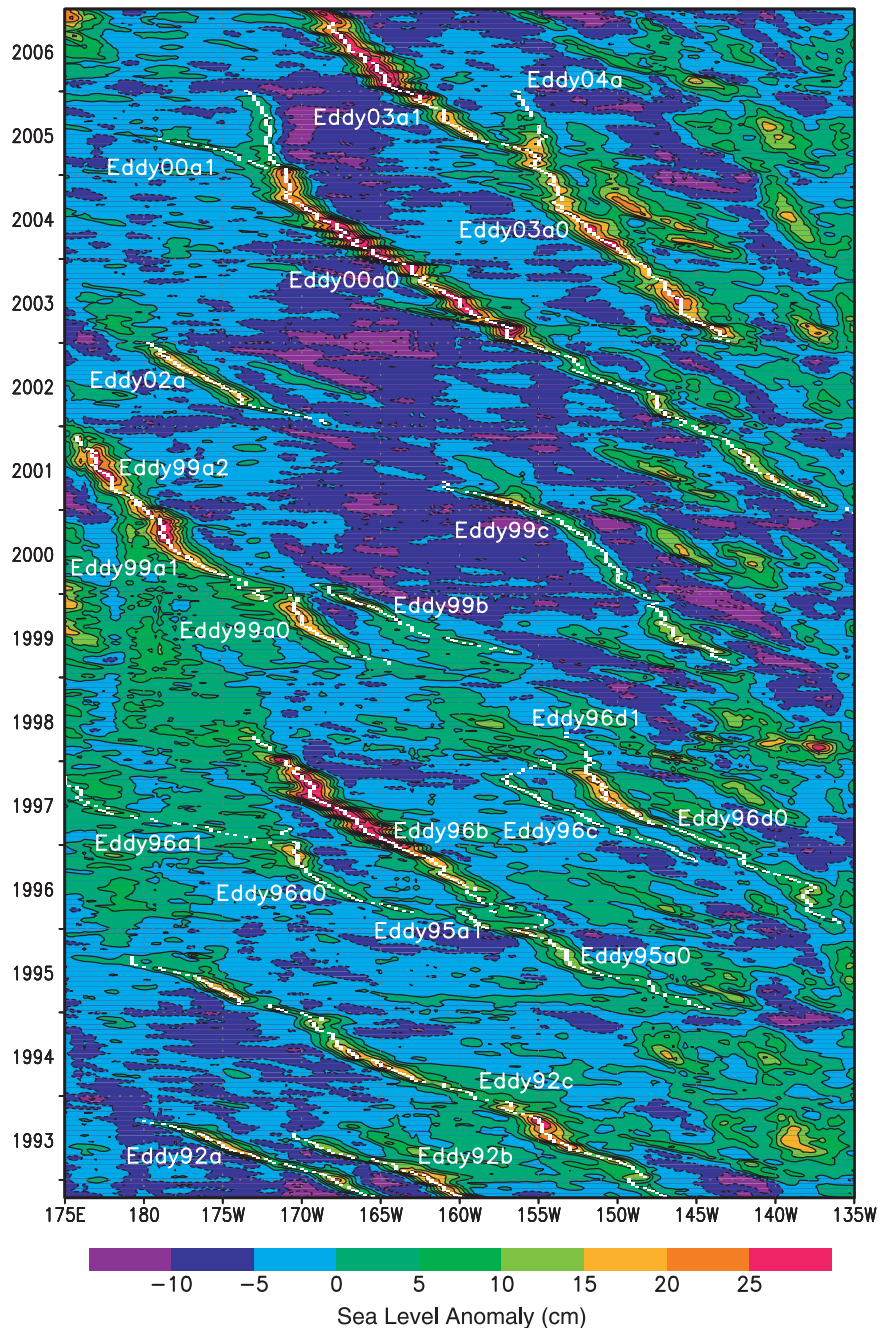


FIG. 3. Longitude–time diagram of the SLA along the northern boundary of the Pacific Ocean. The SLA was averaged within 2° south of the 1000-m depth contour (see Fig. 1). White dots indicate the locations of eddies shown in Fig. 2 excluding eddies more than 2° south of the 1000-m depth contour.

latter warmer water, located in the eddy (< 70 km), was similar to the Alaska Current Water, which was observed in the high velocity core of the AS (Musgrave et al. 1992).

At depths between 150 and 250 m, water at the eddy center is colder than the water 25–50 km away from the

eddy center. This was also true on isopycnals between 25.8 and $26.4 \sigma_\theta$ (Fig. 4d), in contrast with Tabata (1982), who indicated that waters at the center of Sitka eddies in the eastern Gulf of Alaska were isopycnally warmer than those away from the center in a density range of 25.6 – $26.6 \sigma_\theta$. Two profiles closest to the eddy center (red

Eddy00a

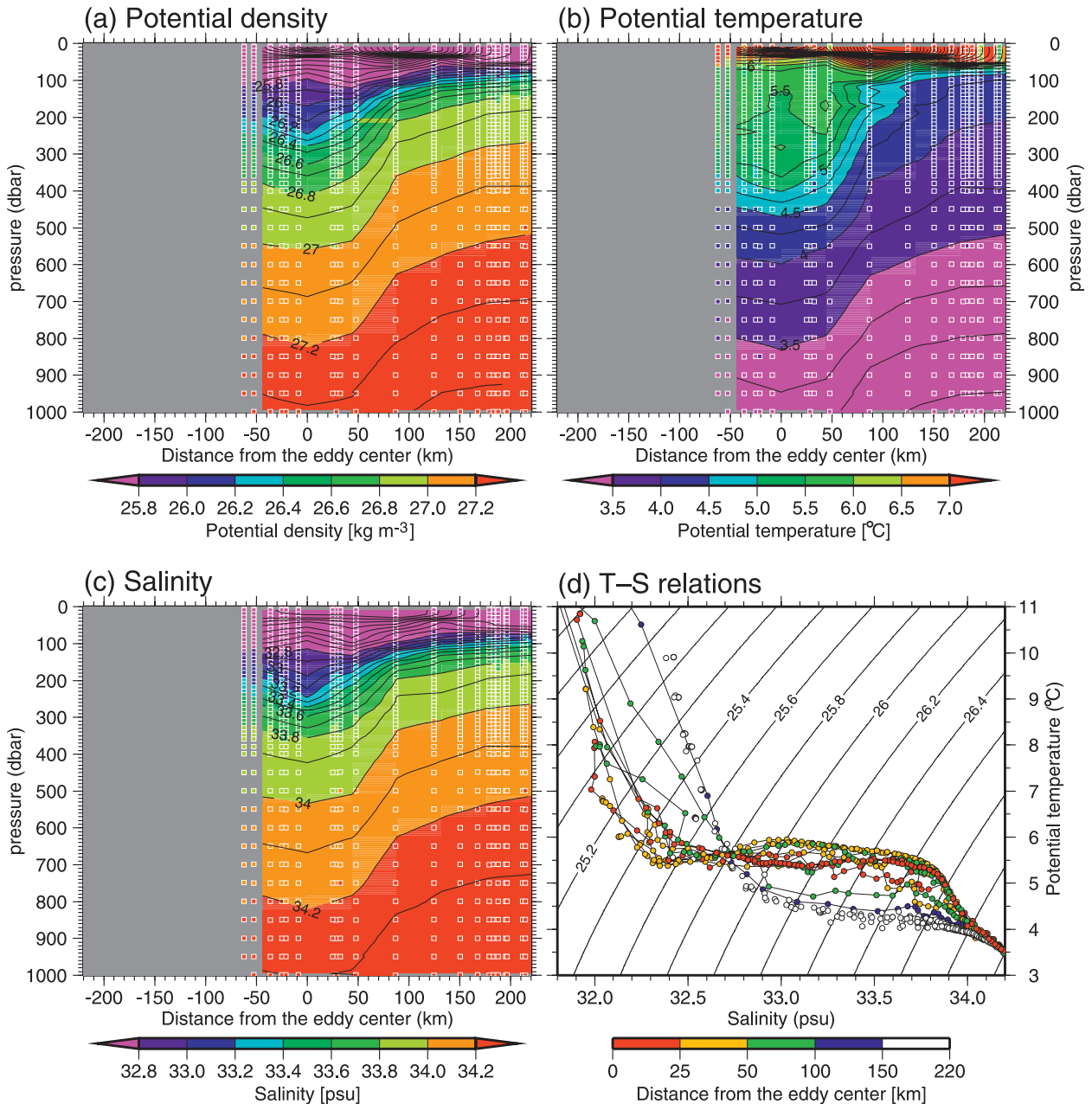


FIG. 4. Composite cross sections of (a) potential density, (b) potential temperature, and (c) salinity, and (d) a T-S diagram for eddy 00a based on Argo float observations from 15 May (159.25°W) to 10 Dec 2003 (163.5°W). Colored squares with white outline in (a)–(c) represent water properties observed by Argo floats, and background colors and contours denote properties horizontally box averaged with a width of 44 km. Horizontal axes in (a)–(c) are the radial distance from the eddy center, which is positive (negative) when an Argo float is located east (west) of the eddy center. Positions of eddy centers are determined from satellite SLA data. Color in (d) represents the distance from the eddy center. Contour intervals are (a) 0.1 kg m⁻³, (b) 0.25°C below 7°C and 0.5°C above 7°C, and (c) 0.1 psu.

circles with a temperature of ~5.5°C between 26.0 and 26.6 σ_θ) have a weak temperature minimum between 26.1 and 26.2 σ_θ . The subsurface temperature minimum observed in the Gulf of Alaska in 2003 is considered to

be formed in the mixed layer in the 2001/02 winter and to survive for more than 1 yr (Ueno et al. 2005, 2007). Eddy 00a was located at the head of the Gulf of Alaska in the 2001/02 winter (Fig. 2). This suggests that this

Eddy03a

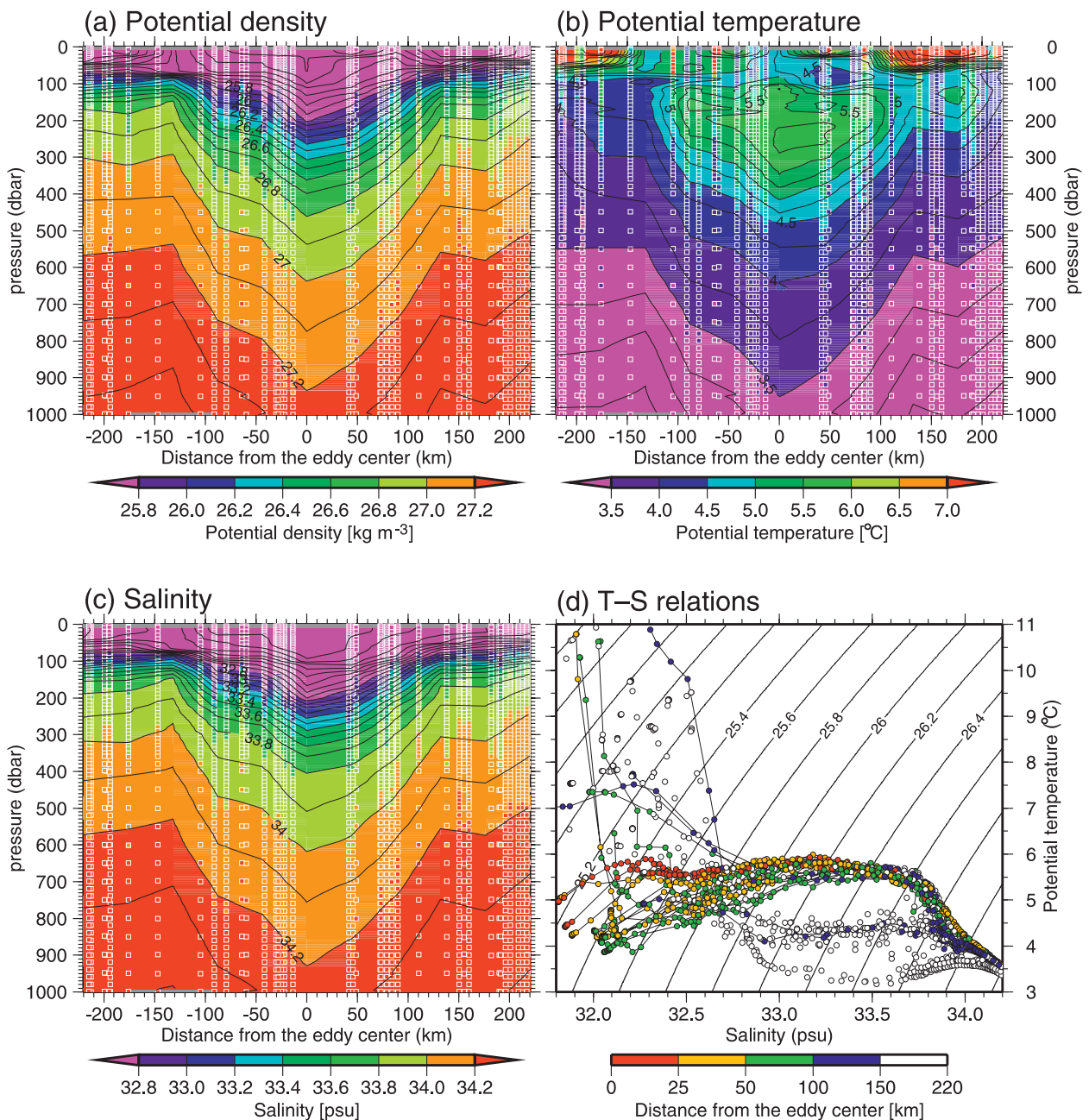


FIG. 5. Same as in Fig. 4, but for eddy 03a from 11 Jan (164°W) to 27 Dec 2006 (169.5°W).

eddy transported water formed in the 2001/02 winter mixed layer at the head of the Gulf of Alaska to the area of 159°–164°W where it was sampled by an Argo float.

Eddy 03a (Yakutat eddy) was observed at 164°–170°W in 2006 by three Argo floats while propagating southwestward in the AS (Fig. 5). At depths greater than 250 m, isopycnals, isotherms, and isohalines lowered to the

eddy center within ~100 km from the center. Their depths were almost constant in the area farther than 150 km, suggesting that the edge of the eddy was located between 100 and 150 km away from the eddy center. This is consistent with the T–S diagram, which indicates that T–S relations of subsurface water in the area farther than 150 km were similar to those of Ridge Domain Water.

Eddy02a

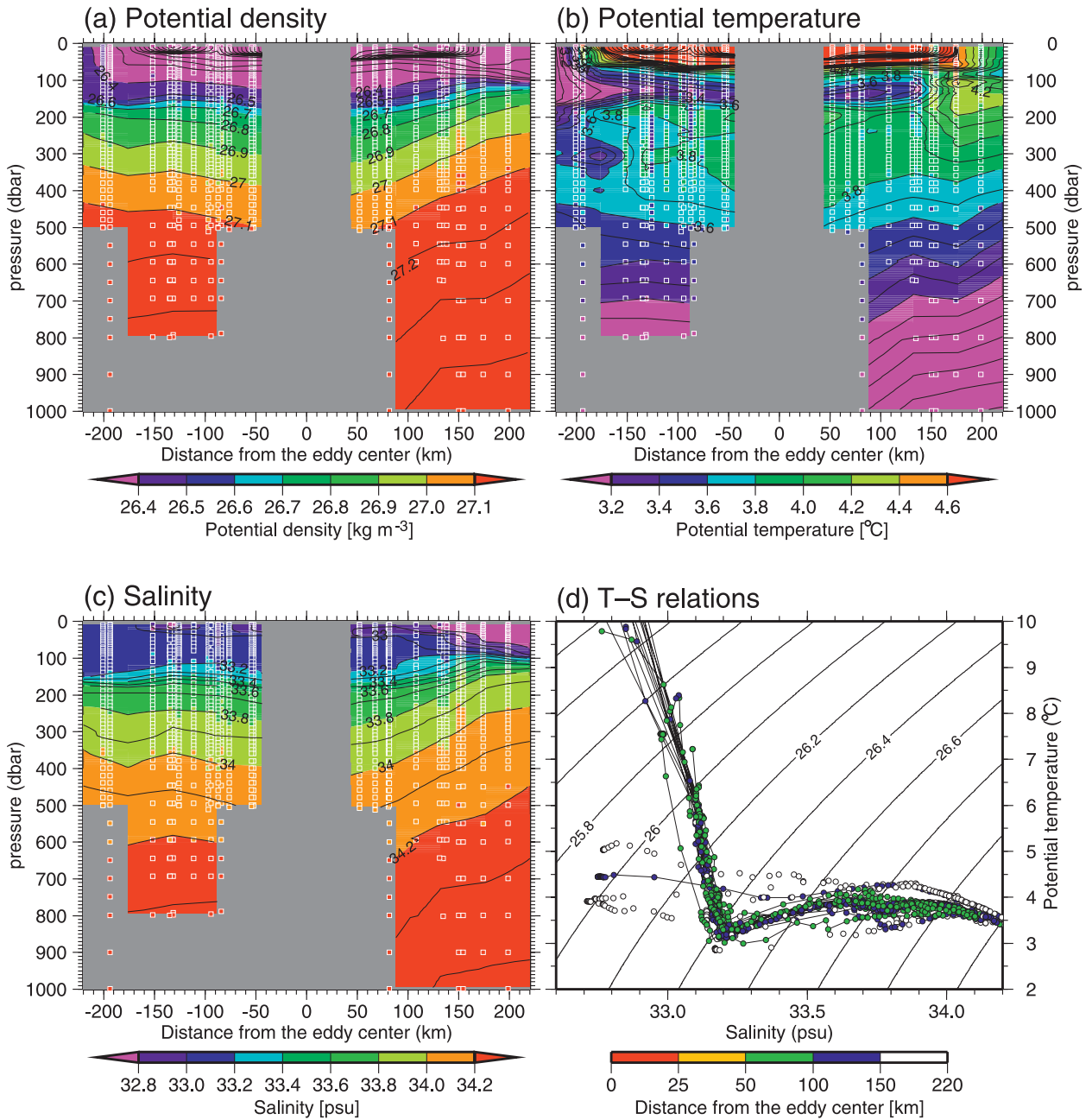


FIG. 6. Same as in Fig. 4, but for eddy 02a from 25 Dec 2002 (179.5°W) to 29 Oct 2003 (176.25°E). The potential temperature contour interval is 0.1°C below 5°C and 0.5°C above 5°C.

Prior to our float observations, hydrographic observations across this eddy were performed 4 times: in May 2003 (eddy center at ~146°W), September 2003 (~147°W), May 2004 (~152°W), and October 2004 (eddy centers at ~154° and ~156°W) (Ladd et al. 2005b, 2007). In May 2003, the water at the eddy center was isopycnally warmer than the surrounding waters in the density

range of 25.4–26.2 σ_{θ} (Ladd et al. 2007). This difference gradually decreased with time, although water at the eddy center was still isopycnally warmer than the surrounding waters in October 2004 (Ladd et al. 2007). Figure 5 shows that the T–S relations near the eddy center (radius < 25 km) are almost indistinguishable from other observations off the center, indicating that

the original water properties at the eddy center were lost by 2006 when Argo floats sampled the eddy.

Eddy 02a (an AS eddy), which formed at 169°W south of the Aleutian Islands in January 2002 and moved to the western subarctic gyre, was observed by three Argo floats between 176°E and 180° from December 2002 to October 2003 (Fig. 6), although all float observations were conducted in the area more than 50 km away from the eddy center. Unlike eddies 00a and 03a, eddy 02a was an isolated eddy detached from the AS when observed by the Argo floats. Near the eddy center, this eddy shows a weak depression of isopycnals and isohalines at depths greater than 200 m, and a weak depression of isotherms at depths greater than 500 m. It is hard to determine the diameter of this eddy.

Since eddy 02a was observed in the western subarctic gyre after it was detached from the AS, we investigated this eddy from the viewpoint of water transport from the AS region to the western subarctic gyre. For this purpose, PV was used as a conservative property as in Yasuda et al. (2000) because T–S relations changed little across the eddy. The thickness of the intermediate layer at $26.5\text{--}26.8\sigma_\theta$ decreases outward from the eddy center; the PVs at the $26.8\sigma_\theta$ isopycnal surface are 1.9, 2.6, and $4.7 \times 10^{-10} \text{ m}^{-1} \text{ s}^{-1}$ in the areas where the distances from the center are less than 100 km, between 100 and 150 km, and 150–220 km (probably out of the eddy), respectively. The PV near the center of eddy 02a was lower than the climatological PV at the same location [$> 3.5 \times 10^{-10} \text{ m}^{-1} \text{ s}^{-1}$; Macdonald et al. (2001); Suga et al. (2004)], but similar to the climatological PV just south of the Aleutian Islands at 180° [$< 2.0 \times 10^{-10} \text{ m}^{-1} \text{ s}^{-1}$ at $26.8\sigma_\theta$; Fig. 3e in Onishi (2001)] and the PVs near the centers of eddies 00a and 03a observed along the AS ($\leq 2.0 \times 10^{-10} \text{ m}^{-1} \text{ s}^{-1}$). These PV values suggest that eddy 02a supplies the deep-sea region of the western subarctic gyre with intermediate water just south of the Aleutian Islands characterized by low PV. This low PV supply might affect the pycnocline structure and thus the upwelling in the western subarctic gyre, which is a key part of the intermediate-water circulation in the subarctic North Pacific (Ueno and Yasuda 2003).

4. Discussion

a. Water exchange among the Aleutian Islands region, the western and central subarctic North Pacific, and the Bering Sea

Okkonen et al. (2003) and Ladd et al. (2005c) indicated that eddies in the AS in the Gulf of Alaska have a significant impact on the heat, freshwater, nutrient (including iron), and biota exchange between the shelf re-

gion and the offshore region by 1) trapping coastal water at the eddy center and 2) changing the slope circulation. We here found that some eddies detached themselves from the AS south of the Aleutian Islands and propagated southwestward, likely exchanging water between the relatively shallow region just around the Aleutian Islands (the Aleutian Islands region) and the offshore region by the mechanism (1) in the central and western subarctic North Pacific. Indeed, eddy 02a was observed to carry low-PV water into the western subarctic gyre. Ten eddies propagating westward in the AS along the Aleutian Islands during 1992–2006 (Fig. 2) might also cause water exchange by the mechanism (2) through disturbing circulation south of the Aleutian Islands.

In addition to the water exchange between the Aleutian Islands region and the western and central subarctic North Pacific, eddies in the AS could affect the water exchange between the North Pacific and the Bering Sea. Okkonen (1996) indicated that an eddy in the Alaskan Stream south of the Amchitka Pass ($\sim 180^\circ$) drove flow through the pass. Therefore, the six eddies that passed near the Amchitka Pass (see Fig. 2) might influence the water exchange between the North Pacific and the Bering Sea.

How much heat and freshwater are transported by an eddy that detached from the AS and entered the western subarctic gyre? Based on the limited hydrographic observations available from Argo floats (section 3c), we roughly estimated the heat and freshwater transports assuming that an eddy with averaged T–S profiles of eddies 00a and 03a followed the same trajectory as eddy 02a, and finally changed to the climatological T–S profiles at the location where eddy 02a decayed.

First, we averaged 17 T–S profiles within 50 km from the center of eddies 00a and 03a (Figs. 4b,c and 5b,c) at each depth between 100 and 1000 m, weighting them by the distance from the eddy center. The top 100-m layer was not used for calculation to avoid the influence of seasonal variations. Assuming that the water column of the averaged T–S profile was transported to 47.5°N and 175.5°E, where eddy 02a decayed, and changed to the climatological annual-mean water column from the *World Ocean Atlas 2005* (Locarnini et al. 2006; Antonov et al. 2006), the heat and freshwater released along the trajectory from the AS region to the western subarctic gyre were estimated to be $3.4 \times 10^{19} \text{ J}$ and $5.0 \times 10^{10} \text{ m}^3$, respectively. These values are almost the same as the heat and freshwater transports of $3 \times 10^{19} \text{ J}$ and $5 \times 10^{10} \text{ m}^3$ released to the deep-sea region of the Gulf of Alaska by a typical Haida eddy (Crawford 2005).

Assuming that an AS eddy releases its heat and salt in the $5^\circ \times 5^\circ$ area of the western subarctic gyre in a year, its heat and freshwater fluxes are evaluated as 5.4 W m^{-2}

and 0.26 m yr^{-1} , respectively. These are comparable to NCEP–NCAR surface net heat and freshwater fluxes ($10\text{--}20 \text{ W m}^{-2}$ and $0.5\text{--}1.0 \text{ m yr}^{-1}$ into the ocean) along the trajectory of eddy 02a in the western subarctic gyre. Since AS eddies did not enter the western subarctic gyre every year, they might affect the interannual variation of temperature and salinity in the western subarctic gyre.

b. Formation and evolution mechanisms of eddies in the AS

Thomson (1972) investigated the AS analytically via steady, barotropic frictional theory and indicated that the frictional boundary layer (the AS) would separate from the coast when the planetary vorticity variation could not balance the diffusion of negative vorticity from the boundary as the result of the changing zonal orientation of the boundary. Based on his theory, separation of the AS more likely occurs where AS flows nearly zonally and when the wind stress curl over the AS is negative. Alaskan Stream eddies formed at $157^{\circ}\text{--}169^{\circ}\text{W}$, where the angle between the latitude lines and the shelf break was small. Therefore, we investigated the wind stress curl along the AS to study the formation mechanism of AS eddies.

Figure 7 shows the 30-day running-mean wind stress curl along the AS between two red contours in Fig. 1 at $175^{\circ}\text{E}\text{--}135^{\circ}\text{W}$ from October 1993 to December 2006, superimposed by the location of the eddies. The standard deviation of the wind stress curl ($\text{curl}\tau$) along the AS at $157^{\circ}\text{--}169^{\circ}\text{W}$ before the running mean was $4.1 \times 10^{-7} \text{ N m}^{-3}$, whose contribution to the vorticity balance ($\text{curl}\tau / \rho h$) in the AS is about 20% of that of the planetary vorticity advection ($\beta v \sin\theta$), assuming that the water density (ρ) is 10^3 kg m^{-3} , the water depth (h) is 5000 m, the latitudinal change of the Coriolis parameter (β) is $1.4 \times 10^{-11} \text{ m}^{-1} \text{ s}^{-3}$, the speed of AS (v) is 10 cm s^{-1} , and the angle between the AS and latitude lines (θ) is 20° . Therefore, the wind stress curl could play a key role in the separation of the AS and thus the formation of AS eddies.

The AS eddies 96a, 96b, 99a, and 99b formed during or just after the negative or weakly positive wind stress curl event (Fig. 7), suggesting that wind stress curl contributed to the formation of these eddies. In addition, ADT data suggest that the AS was relatively weak in 1996 and 1999. Therefore, the contribution of the wind stress curl to the vorticity balance in the AS might be relatively large in those years. On the other hand, eddy 02a formed in the period of strong positive wind stress curl, which likely stabilized the AS. Some other formation mechanisms might contribute to the formation of the eddy.

We next discuss the evolution mechanism of the eddies near 155° and 170°W , as described in section 3b. Eddies 92c, 95a, 96c, 99c, 00a, and 03a were intensified around 155°W , which is close to the exit of the sea valley (southwest of Shelikof Strait; see Fig. 1). From this sea valley, low-salinity and low-density coastal water outflowed to the open ocean near the sea surface (Reed et al. 1986, 1987; Stabeno and Hermann 1996; Stabeno et al. 2004). Such outflow of low-density water from a sea strait (sea valley in this case) to the open ocean could form an anticyclonic eddy. Di Lorenzo et al. (2005) indicated that warm and freshwater outflows from Hecate Strait east of the Queen Charlotte Islands generated small patches of buoyant water in the area west of the islands. The difference in density between the core of the patches and the ambient water intensified and sustained the anticyclonic circulation of these patches, which then merged to generate a larger eddy, the Haida eddy (Di Lorenzo et al. 2005). Based on their eddy formation and intensification mechanism, low-salinity surface water outflow around 155°W indicated by previous studies might intensify eddies propagating southwestward along the AS. For instance, some surface drifting buoys coming out of the sea valley were trapped by an eddylike feature in the AS (Stabeno and Hermann 1996; Stabeno et al. 2004).

The longitude of 170°W is located just west of Samalga Pass, which is the easternmost Aleutian pass with a sill depth greater than 100 m. Water properties just south of the Aleutian Islands changed westward beyond the pass due to the southward flow from the Bering Sea through the passes west of Samalga (Favorite 1974; Ladd et al. 2005a). At the Amukta Pass around 172°W , for example, southward flow of $0.4 \pm 0.2 \text{ Sv}$ ($1 \text{ Sv} \equiv 10^6 \text{ m}^3 \text{ s}^{-1}$) was observed on the western side of the pass (Reed and Stabeno 1997). Waters in the Bering Sea and the passes along the Aleutian Islands are characterized by low PV compared with those in the North Pacific (e.g., Suga et al. 2004), suggesting that low-PV water outflows from the Bering Sea to the south. A theoretical study indicated that such low-PV outflow from a sea strait formed an anticyclonic eddy when the outflow exceeded a critical volume (Kubokawa 1991). Thus, low potential vorticity outflows from the Bering Sea likely intensify eddies in the AS around 170°W . This situation is similar to that along the Kuril Islands discussed by Yasuda et al. (2000). They suggested that Kuroshio warm-core rings that had propagated northeastward were arrested near the Bussol' Strait along the Kuril Islands and were amplified with the supply of low-PV water from the Okhotsk Sea. Furthermore, eddies seem to detach preferentially at both longitudes of 155° and 170°W , as described in section 3b. This might be

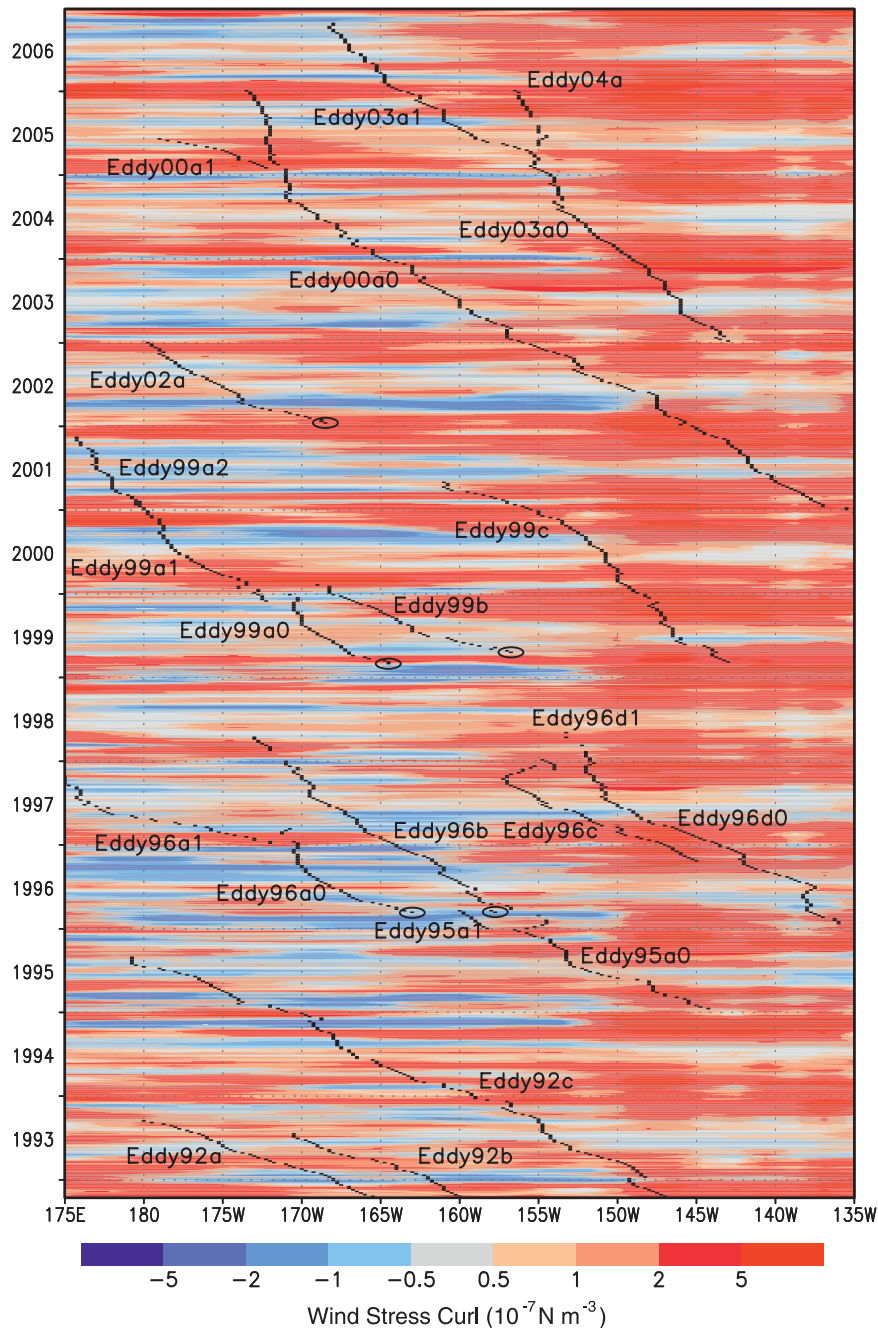


FIG. 7. Longitude–time diagram of the wind stress curl averaged within 2° south of the 1000-m depth contour (see Fig. 1). The black dots are the same as the white dots in Fig. 3. Locations of AS eddy formation are encircled by ellipses.

related to the intensification of eddies at these longitudes.

c. Eddy propagation speed in the AS

Finally, we discuss the propagation speeds of eddies in the AS, using eddy trajectories shown in Fig. 2. The southwestward alongshore eddy propagation speed ranged

from -0.5 to 7.0 km day^{-1} , and was 2.0 km day^{-1} on average. Since Okkonen et al. (2003) indicated that faster eddies tended to propagate closer to the shelf along the AS in the Gulf of Alaska, we first investigate the relation between the topographic slope and the eddy speed.

In Fig. 8a, the principal ellipse of variance (see Freeland et al. 1975) is elongated in the upper-right to bottom-left

direction, and the principal axis is represented by $y = 0.09x + 0.37$, where y is the eddy speed (km day^{-1}) and x is the bottom slope (m km^{-1}), indicating that a faster eddy propagation speed is associated with a steeper bottom slope. The correlation coefficient is 0.58. This suggests that eddies along the AS are affected by the topographic beta term. It is important to note that the southwestward eddy speeds in Fig. 8 were the 8-week-averaged speeds, and thus it was hard to determine the equivalent number of degrees of freedom.

The dispersion relation of the topographic planetary wave is independent of stratification when the wavelength is long compared to the internal Rossby radius of deformation, assuming zero planetary beta and constant stratification (LeBlond and Mysak 1978, section 20). The wavelengths of eddies in the AS are $O(100 \text{ km})$ (Crawford et al. 2000), which is long compared with the internal Rossby radii of deformation in the AS region of 10–20 km (Emery et al. 1984; Chelton et al. 1998). Therefore, from the dispersion relation of a topographic planetary wave (LeBlond and Mysak 1978), the along-shore phase speed of a topographic planetary wave, C_{TPW} , is written as

$$C_{\text{TPW}} = -f \frac{H_\eta}{H} \frac{1}{k^2 + l^2}, \quad (1)$$

where f is the Coriolis parameter; H is the water depth; H_η is the bottom slope normal to the 1000-m depth contour; and k and l are the wavenumbers along and normal to the 1000-m depth contour, respectively. Substituting the wavelength of 100 km, the water depth of 5000 m, and the Coriolis parameter at 55°N , we obtained the relation between the bottom slope (m km^{-1}) and the topographic wave speed (km day^{-1}) of $C_{\text{TPW}} = 0.26 H_\eta$. The slope of 0.26 is about 3 times as large (fast) as the slope of principal axis in Fig. 8a, suggesting that some other mechanisms slow down the eddy propagation speed. As discussed in sections 3b and 4b, eddies stopped propagating for a while and amplified at some longitudes, which would indicate that nonlinear effect of eddy intensification was dominant during the period. This nonlinear effect might be one of the mechanisms involved in slowing down the eddy speed.

Higher eddy propagation speed was associated with lower SLAs at the eddy center, with a correlation coefficient of -0.31 (Fig. 8b). This is consistent with Fig. 3, which shows that eddies were intensified while they slowed down. Figure 3 also implies that eddies with high SLA tend to occupy a wide longitudinal range, suggesting that large eddies propagate slowly. This contradicts the dispersion relation of topographic planetary waves, where the phase speed is independent of SLA and increases with eddy size [see Eq. (1)]. It is thus

suggested that nonlinear effects play an important role in the eddy propagation along the AS, possibly reducing the propagation speed as demonstrated above.

We further examined the relations between the eddy speed and the surface AS velocity, although the AS velocity calculated from ADT data had relatively large errors due to the closeness to the shelf break (Ducet et al. 2000). Figure 8c shows that the mean eddy speed (2.0 km day^{-1}) is much slower than mean surface AS velocity of 13.2 km day^{-1} (15.3 cm s^{-1}). The mean eddy speed is also much slower than the mean AS velocity of $O(10 \text{ km day}^{-1})$ at depths shallower than 1000 m across 180° (Onishi 2001), indicating that eddies are not just advected by the AS. Furthermore, eddy speed is hardly correlated to the AS surface velocity (correlation coefficient = 0.19). This could be mainly attributed to the effects of an AS velocity change to the direction normal to the coast, which changes the background PV gradient. Okkonen (1993) indicated that the effects of this background PV gradient on the eddy propagation speed and the effects of advection due to the background current field could cancel one another for the Bering Slope Current. He also indicated that the ratio of the former effects to the latter is represented by L^2/λ^2 , where L is the width of the current and λ is the wavelength of the eddy. Since L and λ are almost the same order in the AS, the two effects can cancel out, possibly resulting in the eddy propagation speed being much slower than the AS velocity and the low correlation between the eddy speed and the AS velocity. Baroclinic mean flow of the AS, which also changes the background PV gradient (Killworth et al. 1997), might contribute to the eddy speed as well.

The eddy propagation speed over a flat bottom is next discussed briefly. From the principal axis in Fig. 8a, the best-fit along-coast propagation speed of eddies over a flat bottom ocean was estimated to be 0.37 km day^{-1} . This value is almost the same as the propagation speed predicted at the latitude of the AS for a linear, non-dispersive planetary wave of $0.1\text{--}0.4 \text{ km day}^{-1}$ from the internal Rossby radius of deformation in the AS region of 10–20 km (Emery et al. 1984; Chelton et al. 1998).

We finally discuss the seasonal and interannual variations of the eddy speed, SLA, and the AS velocity (Fig. 8d), averaging values in Figs. 8b and 8c in month and year. The eddy speed is high in winter and spring and low in summer and fall. The AS velocity is also high in winter and low in summer as indicated by Strub and James (2002), who analyzed SLA data combined with tide gauge data and indicated that the AS surface velocity took a minimum in summer in coincidence with a weak Aleutian low. The correlation coefficient between the eddy speed and the AS speed is 0.68. The AS might

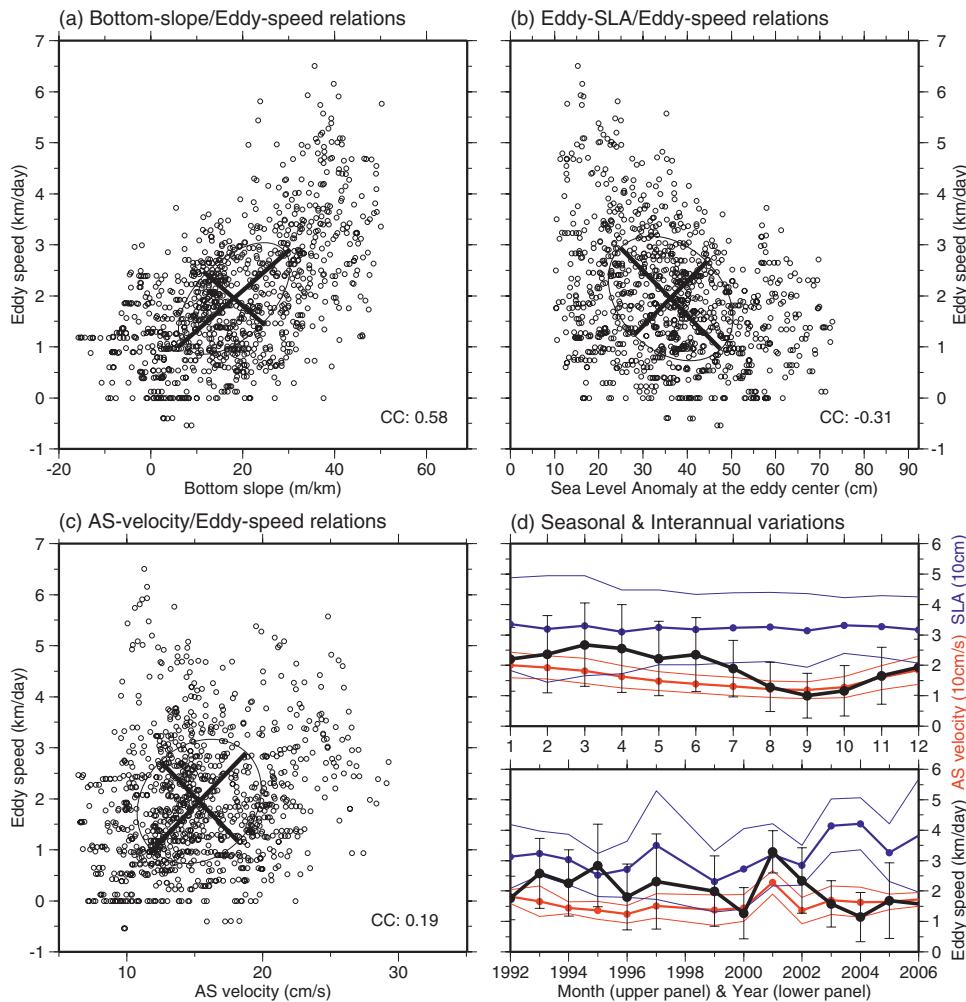


FIG. 8. Scatterplot of (a) bottom slope normal to the 1000-m depth contour (Fig. 1), (b) the SLA at the eddy center, (c) the surface AS velocity along the 1000-m depth contour, and the eddy speed along the 1000-m depth contour, superimposed by principal ellipses of the variance. (d) (top) Seasonal and (bottom) interannual variation of eddy speed along the 1000-m depth contour [black line with error (one standard deviation) bars], surface AS velocity along 1000-m depth contour (red lines), and SLA at the eddy center (blue lines). Thin red (blue) lines denote the AS velocity (SLA) ± 1 standard deviation.

accelerate/decelerate the eddy propagation on a seasonal basis, although it is difficult to discuss the causality from Fig. 8d. On the other hand, the eddy SLA is almost constant throughout the year compared with its original variability (Fig. 8b), and has no relation with the eddy speed (correlation coefficient is -0.08).

No significant relation was detected between interannual variations in eddy speed, AS velocity, and SLA (Fig. 8d, bottom panel). The correlation coefficients between the eddy speed and SLA, and eddy speed and AS velocity, were -0.38 and 0.28 , respectively. This is probably because interannual variations in eddy speed and SLA depend on the characteristics (e.g., trajectory) of each eddy, as suggested by Henson and Thomas (2008),

who investigated the relation between interannual variations in a number of individual eddies, SLAs, and eddy speeds along the AS between 142.5° and 160°W .

5. Conclusions

We investigated anticyclonic eddies in the Alaskan Stream (AS) using sea level anomaly (SLA) data during 1992–2006 and hydrographic data obtained by Argo float observations during 2001–06. Fifteen long-lived eddies were identified and categorized based on their area of first appearance.

Eddies 92a, 92b, and 92c were present from the beginning of the altimetry observations, and propagated

downstream along the AS without detachment from the AS. Eddies 96d, 00a, and 04a were first observed along the northeastern Gulf of Alaska off Sitka (Sitka eddies), propagating westward along the Alaska Current and the AS. Eddy 00a was observed by Argo floats around 160°W and water at the eddy center was isopycnally colder than the water away from the center between 25.8 and 26.4 σ_θ , in contrast to Sitka eddies in the eastern Gulf of Alaska observed in the previous studies. Eddies 95a, 96c, 99c, and 03a formed at the head of the Gulf of Alaska near Yakutat (Yakutat eddies) and propagated westward along the AS. Argo float observations of eddy 03a indicated that the original water properties at the eddy center were lost by the time of the Argo float observations. All Sitka and Yakutat eddies stayed east of 180°. Some of them detached from the AS, but all of them moved less than 5° in longitude after their detachment.

Eddies 96a, 96b, 99a, 99b, and 02a formed along the AS between 157° and 169°W and we call these eddies Alaskan Stream eddies. These eddies, except eddy 99b, propagated beyond 180° and reached the western subarctic gyre. The AS eddies, except eddy 02a, formed when the wind stress curl was either negative or weakly positive, likely causing AS separation. Eddy 02a was observed by Argo floats in the western subarctic gyre after it detached from the AS. The observations suggested that the eddy provided the western subarctic gyre with low-PV intermediate water, as well as heat and freshwater, in the area just south of the Aleutian Islands.

Comparisons of westward eddy propagation speeds in the AS with bottom slope, AS velocity, and SLA showed that the bottom slope effects dominated, with faster propagation over steeper slopes. The eddy propagation speed was slower than that predicted by the topographic planetary wave dispersion relation. This is probably because of nonlinear effects due to, for example, eddy intensification associated with water input from the Shelikof Strait sea valley and the Bering Sea.

Acknowledgments. The authors thank two anonymous reviewers and L. D. Talley, the editor of this manuscript. Their comments were very helpful and improved this paper. Most of this work was done while H. Ueno was staying at the Institute of Ocean Sciences (IOS) as a visiting scientist. The altimeter products were produced by SSALTO/DUACS and distributed by AVISO with support from CNES. The Argo float data used in this study were collected and made freely available by the International Argo Project and the national programs that contribute to it (information online at <http://www.argo.ucsd.edu> and <http://argo.jcommops.org>). Argo is a pilot program of the Global

Ocean Observing System. H. Ueno was partially supported by the Japanese Ministry of Education, Culture, Sports, Science and Technology [KAKENHI, Grant-in-Aid for Young Scientists (B) 20740277].

REFERENCES

- Antonov, J. I., R. A. Locarnini, T. P. Boyer, A. V. Mishonov, and H. E. Garcia, 2006: *Salinity*. Vol. 2, *World Ocean Atlas 2005*, NOAA Atlas NESDIS 62, 182 pp.
- Argo Science Team, 2001: The global array of profiling floats. *Observing the Oceans in the 21st Century*, C. J. Koblinsky and N. R. Smith, Eds., GODAE Project Office, Bureau of Meteorology, 248–258.
- AVISO, 2007: SSALTO/DUACS user handbook: (M)SLA and (M)ADT near-real time and delayed time products. Version 1, Revision 8, CLS, Ramonville St-Agne, France, 42 pp. [Available from CLS, 8-10 Rue Hermès, Parc Technologique du Canal, 31526 Ramonville St-Agne, France.]
- Boyd, P. W., C. S. Wong, J. Merrill, F. Whitney, J. Snow, P. J. Harrison, and J. Gower, 1998: Atmospheric iron supply and enhanced vertical carbon flux in the NE subarctic Pacific: Is there a connection? *Global Biogeochem. Cycles*, **12**, 429–441.
- , and Coauthors, 2004: The decline and fate of an iron-induced subarctic phytoplankton bloom. *Nature*, **428**, 549–553.
- Chelton, D. B., R. A. de Szoeke, M. G. Schlax, K. E. Naggar, and N. Siwertz, 1998: Geographical variability of first baroclinic Rossby radius of deformation. *J. Phys. Oceanogr.*, **28**, 433–460.
- , M. G. Schlax, R. M. Samelson, and R. A. de Szoeke, 2007: Global observations of large oceanic eddies. *Geophys. Res. Lett.*, **34**, L15606, doi:10.1029/2007GL030812.
- Crawford, W. R., 2002: Physical characteristics of Haida eddies. *J. Oceanogr.*, **58**, 703–713.
- , 2005: Heat and fresh water transport by eddies into the Gulf of Alaska. *Deep-Sea Res. II*, **52**, 893–908.
- , and F. Whitney, 1999: Mesoscale eddies swirl with data in Gulf of Alaska ocean. *Eos, Trans. Amer. Geophys. Union*, **80**, 365–370.
- , J. Y. Cherniawsky, and M. G. G. Foreman, 2000: Multi-year meanders and eddies in the Alaskan Stream as observed by TOPEX/Poseidon altimeter. *Geophys. Res. Lett.*, **27**, 1025–1028.
- , P. J. Brickley, T. D. Peterson, and A. C. Thomas, 2005: Impact of Haida eddies on chlorophyll distribution in the eastern Gulf of Alaska. *Deep-Sea Res. II*, **52**, 975–989.
- , —, and A. C. Thomas, 2007: Mesoscale eddies dominate surface phytoplankton in northern Gulf of Alaska. *Prog. Oceanogr.*, **75**, 287–303.
- Di Lorenzo, E., M. G. G. Foreman, and W. R. Crawford, 2005: Modelling the generation of Haida eddies. *Deep-Sea Res. II*, **52**, 853–873.
- Ducet, N., P. Y. Le Traon, and G. Reverdin, 2000: Global high-resolution mapping of ocean circulation from TOPEX/Poseidon and ERS-1 and -2. *J. Geophys. Res.*, **105** (C8), 19 477–19 498.
- Emery, W. J., W. G. Lee, and L. Magaard, 1984: Geographic and seasonal distribution of Brunt–Väisälä frequency and Rossby radii in the North Pacific and North Atlantic. *J. Phys. Oceanogr.*, **14**, 294–317.
- Favorite, F., 1974: Flow into the Bering Sea through Aleutian island passes. *Oceanography of the Bering Sea with Emphasis on Renewable Resources*, D. W. Hood and E. J. Kelley, Eds.,

- Institute of Marine Science, University of Alaska—Fairbanks, 3–37.
- Freeland, H. J., P. B. Rhines, and T. Rossby, 1975: Statistical observations of the trajectories of neutrally buoyant floats in the North Atlantic. *J. Mar. Res.*, **33**, 383–404.
- Gower, J. F. R., 1989: Geosat altimeter observations of the distribution and movement of sea-surface height anomalies in the north-east Pacific. *Proc. Oceans 89: The Global Ocean*, Seattle, WA, IEEE, 977–981.
- Harrison, P. J., P. W. Boyd, D. E. Varela, S. Takeda, A. Shiimoto, and T. Odate, 1999: Comparison of factors controlling phytoplankton productivity in the NE and NW subarctic Pacific gyres. *Prog. Oceanogr.*, **43**, 205–234.
- Henson, S. A., and A. C. Thomas, 2008: A census of oceanic anticyclonic eddies in the Gulf of Alaska. *Deep-Sea Res. I*, **55**, 163–176.
- Johnson, W. K., L. A. Miller, N. E. Sutherland, and C. S. Wong, 2005: Iron transport by mesoscale Haida eddies in the Gulf of Alaska. *Deep-Sea Res. II*, **52**, 933–953.
- Kalnay, E., and Coauthors, 1996: The NCEP/NCAR 40-Year Reanalysis Project. *Bull. Amer. Meteor. Soc.*, **77**, 437–471.
- Killworth, P. D., D. B. Chelton, and R. A. de Szoeke, 1997: The speed of observed and theoretical long extratropical planetary waves. *J. Phys. Oceanogr.*, **27**, 1946–1966.
- Kubokawa, A., 1991: On the behavior of outflows with low potential vorticity from a sea strait. *Tellus*, **43A**, 168–176.
- Ladd, C., 2007: Interannual variability of the Gulf of Alaska eddy field. *Geophys. Res. Lett.*, **34**, L11605, doi:10.1029/2007GL029478.
- , G. L. Hunt Jr., C. W. Mordy, S. A. Salo, and P. J. Stabeno, 2005a: Marine environment of the eastern and central Aleutian Islands. *Fish. Oceanogr.*, **14** (S1), 22–38.
- , N. B. Kachel, C. W. Mordy, and P. J. Stabeno, 2005b: Observations from a Yakutat eddy in the northern Gulf of Alaska. *J. Geophys. Res.*, **110**, C03003, doi:10.1029/2004JC002710.
- , P. J. Stabeno, and E. D. Cokelet, 2005c: A note on cross-shelf exchange in the northern Gulf of Alaska. *Deep-Sea Res. I*, **52**, 667–679.
- , C. W. Mordy, N. B. Kachel, and P. J. Stabeno, 2007: Northern Gulf of Alaska eddies and associated anomalies. *Deep-Sea Res. I*, **54**, 487–509.
- LeBlond, P. H., and L. A. Mysak, 1978: *Waves in the Ocean*. Elsevier, 602 pp.
- Le Traon, P. Y., Y. Faugere, F. Hernandez, J. Dorandeu, F. Mertz, and M. Ablain, 2003: Can we merge GEOSAT follow-on with TOPEX/Poseidon and ERS-2 for an improved description of the ocean circulation? *J. Atmos. Oceanic Technol.*, **20**, 889–895.
- Locarnini, R. A., A. V. Mishonov, J. I. Antonov, T. P. Boyer, and H. E. Garcia, 2006: *Temperature*. Vol. 1, *World Ocean Atlas 2005*, NOAA Atlas NESDIS 61, 182 pp.
- Macdonald, A. M., T. Suga, and R. G. Curry, 2001: An isopycnally averaged North Pacific climatology. *J. Atmos. Oceanic Technol.*, **18**, 394–420.
- Mackas, D. L., and M. Galbraith, 2002: Zooplankton community composition along the inner portion of Line P during the 1997–1998 El Niño event. *Prog. Oceanogr.*, **54**, 423–437.
- Martin, J. H., R. M. Gordon, S. Fitzwater, and W. W. Brokenow, 1989: Vertex: Phytoplankton/iron studies in the Gulf of Alaska. *Deep-Sea Res.*, **30**, 649–680.
- Musgrave, D. L., T. J. Weingartner, and T. C. Royer, 1992: Circulation and hydrography in the northwestern Gulf of Alaska. *Deep-Sea Res.*, **39A**, 1499–1519.
- National Geophysical Data Center, cited 2006: 2-minute gridded global relief data (ETOPO2v2). [Available online at <http://www.ngdc.noaa.gov/mgg/fliers/06mgg01.html>.]
- Oka, E., L. D. Talley, and T. Suga, 2007: Temporal variability of winter mixed layer in the mid- to high-latitude North Pacific. *J. Oceanogr.*, **63**, 293–307.
- Okkonen, S. R., 1992: The shedding of an anticyclonic eddy from the Alaskan Stream as observed by the Geosat altimeter. *Geophys. Res. Lett.*, **19**, 2397–2400.
- , 1993: Observations of topographic planetary waves in the Bering Slope Current using the Geosat altimeter. *J. Geophys. Res.*, **98** (C12), 22 603–22 613.
- , 1996: The influence of an Alaskan Stream eddy on flow through Amchitka Pass. *J. Geophys. Res.*, **101** (C4), 8839–8851.
- , G. A. Jacobs, E. J. Metzger, H. E. Hurlburt, and J. F. Shriver, 2001: Mesoscale variability in the boundary currents of the Alaska Gyre. *Cont. Shelf Res.*, **21**, 1219–1236.
- , T. J. Weingartner, S. L. Danielson, D. L. Musgrave, and G. M. Schmidt, 2003: Satellite and hydrographic observations of eddy-induced shelf-slope exchange in the northwestern Gulf of Alaska. *J. Geophys. Res.*, **108**, 3033, doi:10.1029/2002JC001342.
- Onishi, H., 2001: Spatial and temporal variability in a vertical section across the Alaskan Stream and subarctic current. *J. Oceanogr.*, **57**, 79–91.
- , and K. Ohtani, 1999: On seasonal and year-to-year variation in flow of the Alaskan Stream in the central North Pacific. *J. Oceanogr.*, **55**, 597–608.
- Pascual, A., Y. Faugere, G. Larnicol, and P. Y. Le Traon, 2006: Improved description of the ocean mesoscale variability by combining four satellite altimeters. *Geophys. Res. Lett.*, **33**, L02611, doi:10.1029/2005GL024633.
- Reed, R. K., and J. D. Schumacher, 1986: Physical oceanography. *The Gulf of Alaska: Physical Environment and Biological Resources*, D. W. Hood and S. T. Zimmerman, Eds., NOAA, 57–75.
- , and P. J. Stabeno, 1997: Long-term measurements of flow near Aleutian Islands. *J. Mar. Res.*, **55**, 565–575.
- , J. D. Schumacher, and L. S. Incze, 1986: Water properties and circulation in Shelikof Strait, Alaska during 1985. NOAA Tech. Memo. ERL PMEL-68, 35 pp. [NTIS PB87-143053.]
- , —, and —, 1987: Circulation in Shelikof Strait, Alaska. *J. Phys. Oceanogr.*, **17**, 1546–1554.
- Rogachev, K., N. Shlyk, and E. Carmack, 2007: The shedding of mesoscale anticyclonic eddies from the Alaskan Stream and westward transport of warm water. *Deep-Sea Res. II*, **54**, 2643–2656.
- Stabeno, P. J., and A. J. Hermann, 1996: An eddy circulation model for the western Gulf of Alaska shelf. 2. Comparison of results to oceanographic observations. *J. Geophys. Res.*, **101** (C1), 1151–1161.
- , N. A. Bond, A. J. Hermann, N. B. Kachel, C. W. Mordy, and J. E. Overland, 2004: Meteorology and oceanography of the northern Gulf of Alaska. *Cont. Shelf Res.*, **24**, 859–897.
- Strub, P. T., and C. James, 2002: Altimeter-derived surface circulation in the large-scale NE Pacific gyres: Part 1. Seasonal variability. *Prog. Oceanogr.*, **53**, 163–183.
- Suga, T., K. Motoki, Y. Aoki, and A. M. Macdonald, 2004: The North Pacific climatology of winter mixed layer and mode waters. *J. Phys. Oceanogr.*, **34**, 3–22.
- Tabata, S., 1982: The anticyclonic, baroclinic eddy off Sitka, Alaska, in the northeast Pacific Ocean. *J. Phys. Oceanogr.*, **12**, 1260–1282.
- Thomson, R. E., 1972: On the Alaskan Stream. *J. Phys. Oceanogr.*, **2**, 363–371.

- Ueno, H., and I. Yasuda, 2003: Intermediate water circulation in the North Pacific subarctic and northern subtropical regions. *J. Geophys. Res.*, **108**, 3348, doi:10.1029/2002JC001372.
- , E. Oka, T. Suga, and H. Onishi, 2005: Seasonal and interannual variability of temperature inversions in the subarctic North Pacific. *Geophys. Res. Lett.*, **32**, L20603, doi:10.1029/2005GL023948.
- , —, —, —, and D. Roemmich, 2007: Formation and variation of temperature inversions in the eastern subarctic North Pacific. *Geophys. Res. Lett.*, **34**, L05603, doi:10.1029/2006GL028715.
- Whitney, F., and M. Robert, 2002: Structure of Haida eddies and their transport of nutrient from coastal margins into the NE Pacific Ocean. *J. Oceanogr.*, **58**, 715–723.
- Wong, C. S., N. A. D. Waser, Y. Nojiri, F. A. Whitney, J. S. Page, and J. Zeng, 2002: Seasonal cycles of nutrients and dissolved inorganic carbon at high and mid latitudes in the North Pacific Ocean during the Skaugran cruises: Determination of new production and nutrient uptake ratios. *Deep-Sea Res. II*, **49**, 5317–5338.
- Yasuda, I., and Coauthors, 2000: Cold-core anticyclonic eddies south of the Bussol' Strait in the northwestern subarctic Pacific. *J. Phys. Oceanogr.*, **30**, 1137–1157.